Supporting Information for

Pressure effect on thermotropic cubic phases of 1,2-bis(4′-*n*-alkoxybenzoyl)hydrazines

Yoji Maeda,[1] Shoichi Kutsumizu[2,*] and Shinichi Sakurai[3]

[1]*Department of Life Science and Sustainable Chemistry, Faculty of Engineering, Tokyo Polytechnic University, 1583 Iiyama, Atsugi, Kanagawa 243-0297, Japan;* [2]*Department of Chemistry and Biomolecular Science, Faculty of Engineering, Gifu University, 1-1 Yanagido, Gifu 501-1193, Japan;* [3]*Department of Macromolecular Science and Engineering, Graduate School of Science and Technology, Kyoto Institute of Technology, Matsugasaki, Sakyo-ku, Kyoto 606-8585, Japan*

Supplementary Materials (12 pages)

Phase Behavior under Pressure

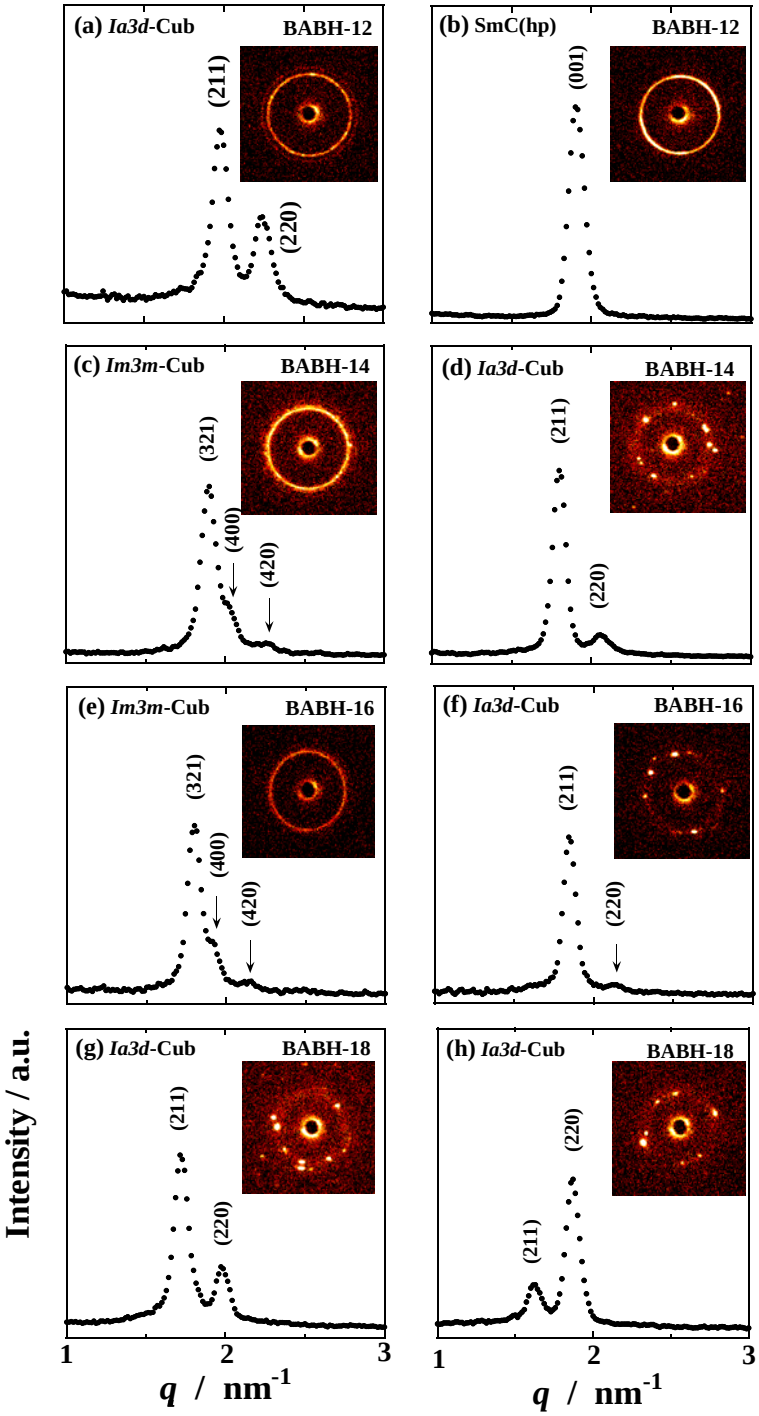

Fig. S1. Selected 1D XRD profiles and 2D images (in insets) recorded (a) at 148 °C (on heating) and 24 MPa and (b) at 146 °C (on cooling) and 30 MPa for BABH-12, (c) at 151 °C (on heating) and 15 MPa and (d) 149 °C (on heating) and 38 MPa for BABH-14, (e) at 145 °C (on heating) and 20 MPa and (f) at 156 °C (on cooling) and 20 MPa for BABH-16, (g) at 144 °C (on cooling) and 30 MPa and (h) at 156 °C (on cooling) and 80 MPa for BABH-18, respectively.

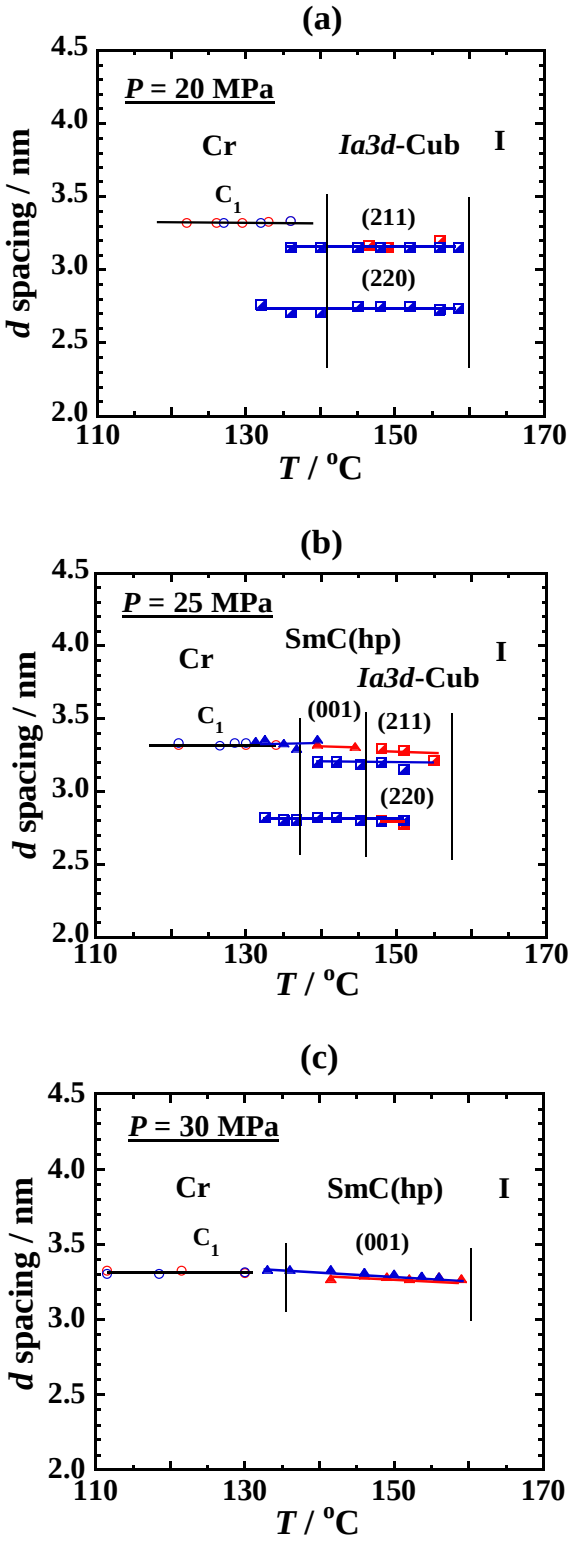

Fig. S2. *d* spacings of observed reflections as a function of temperature for BABH-12 on heating (red) and subsequent cooling (blue) under various pressures of (a) 20, (b) 25, and (c) 30 MPa.

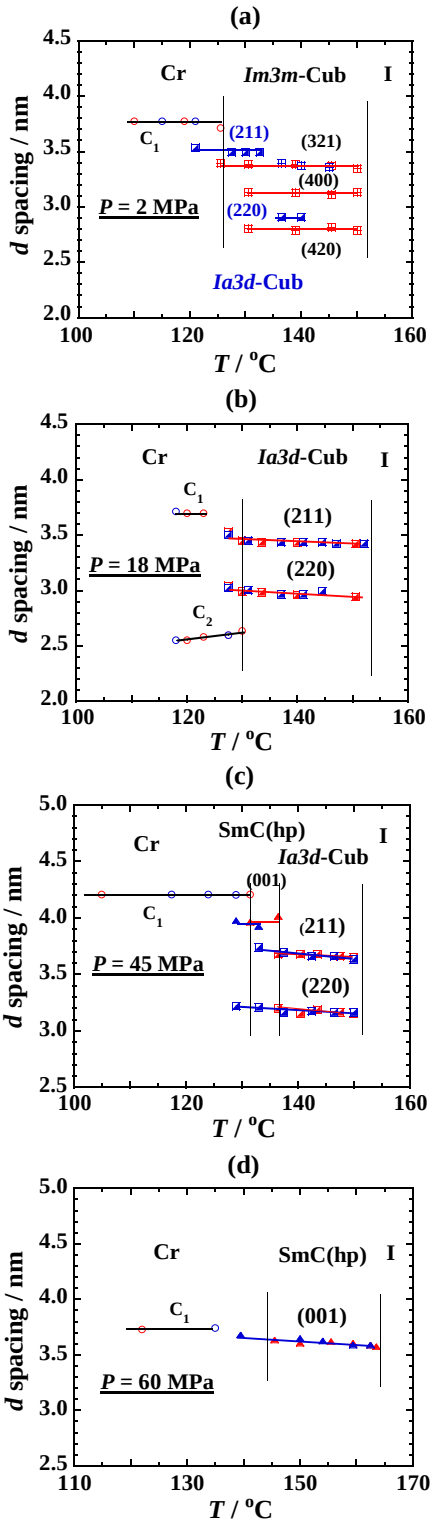

Fig. S3. *d* spacings of observed reflections as a function of temperature for BABH-14 on heating (red) and subsequent cooling (blue) under various pressures of (a) 2, (b) 18, (c) 45, and (d) 60 MPa.

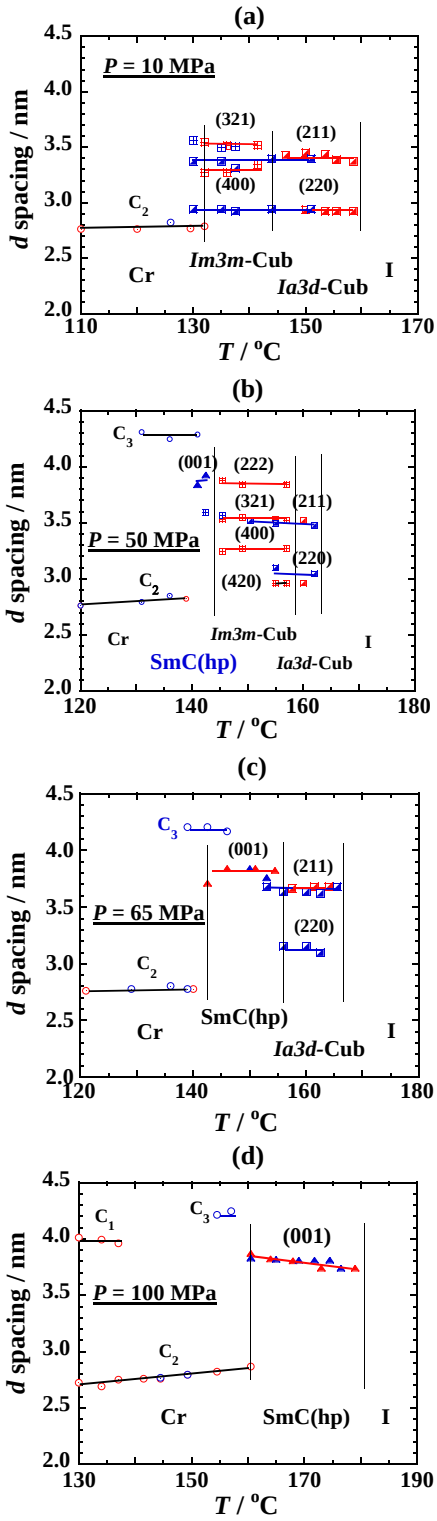

Fig. S4. *d* spacings of observed reflections as a function of temperature for BABH-16 on heating (red) and subsequent cooling (blue) under various pressures of (a) 10, (b) 50, (c) 65, and (d) 100 MPa.

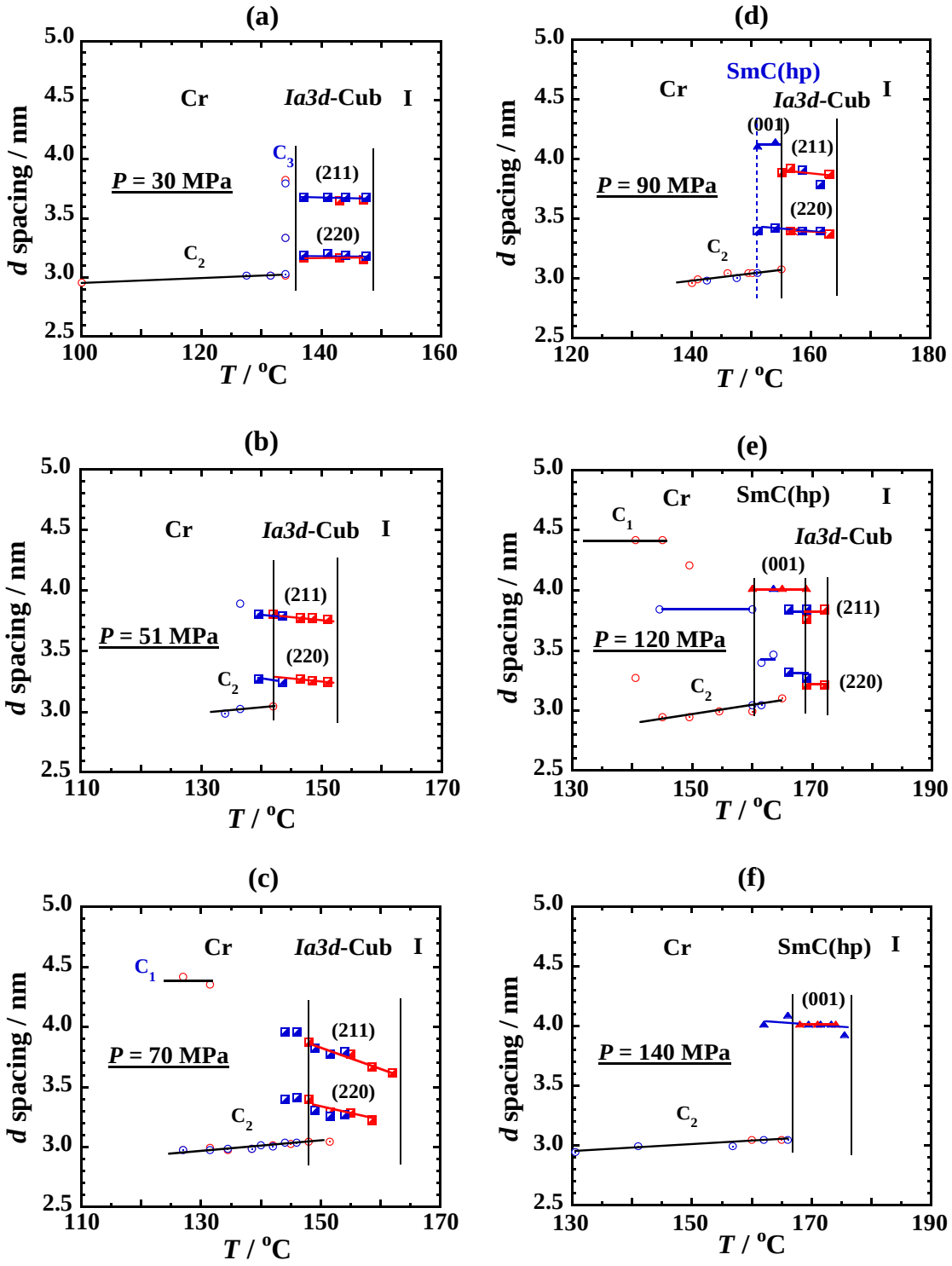

Fig. S5. *d* spacings of observed reflections as a function of temperature for BABH-18 on heating (red) and subsequent cooling (blue) under various pressures of (a) 30, (b) 51, (c) 70, (d) 90, (e) 120, and (f) 140 MPa.

Representative XRD patterns for BABH-12, -14, -16 and -18 under pressures are shown in Figure S1. In the patterns, q is scattering vector defined as $q = (4\pi/\lambda)\sin\theta$ with θ being half the scattering angle.

For the *Ia*3*d*-Cub phase of BABH-12, the common profile of strong (211) and weak (220) reflections was observed in the temperature region 135-155 °C at pressures up to about 24 MPa. The pattern observed at 148 °C and 24 MPa is given in Figure S1a. Above this pressure, in addition to the two reflections, another sharp reflection appears at the lower q side of the *Ia*3*d*-Cub (211) reflection, indicating the formation of the SmC phase (called high-pressure SmC phase and denoted SmC(hp)), and the reflection is assigned to (001). Beyond 26-27 MPa, only the SmC(hp) reflection remained, as exemplified by the pattern at 146 °C and 30 MPa in Figure S1b. The *d* spacings of those reflections and that of the crystalline (Cr) phase are plotted as a function of temperature under various pressures in Figure S2. The *d* spacings of the (211) and (220) reflections of the *Ia*3*d*-Cub phase showed almost no temperature dependence within the experimental errors (Figures S2a and b). On the other hand, the *d* spacing of SmC(hp) (001) reflection slightly decreased with increasing temperature (Figures S2b and c).

Figure S3 shows *d* spacings of observed reflections as a function of temperature for BABH-14 under various pressures. BABH-14 forms an *Im*3*m*-Cub phase at ambient pressure,[1-3] and the Cr – *Im*3*m*-Cub – I phase sequence was retained on heating at pressures up to about 17 MPa.[4,5] The pattern for the *Im*3*m*-Cub phase observed at 151 °C and 15 MPa is given in Figure S1c. The phase behavior on cooling was slightly complicated: At 2 MPa (Figure S3a), both the *Im*3*m*- ((321) reflection) and *Ia*3*d*-Cub phases ((220) reflection) were observed concurrently just below the isotropic liquid on cooling, and after that at lower temperatures, the *Ia*3*d*-Cub phase remained, which was transformed into a crystalline state (C_1 phase). At 16 MPa (the figure not shown here), the Cub phase observed on heating was the *Im*3*m* phase, but on the subsequent cooling, only the *Ia3d* phase was formed throughout the process. The formation of the *Ia*3*d*-Cub phase becomes predominant over that of the *Im*3*m*-Cub phase with increasing pressure on cooling. Beyond 17 MPa, the *Im*3*m*-Cub phase was completely replaced by the *Ia*3*d*-Cub phase, which was observed both on heating and on cooling (Figure 3b for data at 18 MPa). The pattern for the *Ia*3*d*-Cub phase observed at 149 °C and 38 MPa (on heating) is given in Figure S1d. At 45 MPa, as shown in Figure S3c, the SmC(hp) region appeared in the lower temperature side of the *Ia*3*d*-Cub phase, and above about 60 MPa, completely replaced it (Figure S3d for data at 60 MPa).

Figure S4 plots *d* spacings of observed reflections as a function of temperature for BABH-16 under various pressures. At ambient pressure, BABH-16 exhibits two types

of Cub phases, i.e., *Im*3*m* and *Ia*3*d* phases, at low and high temperatures, respectively, and shows the Cr – *Im*3*m*-Cub – *Ia*3*d*-Cub – I phase sequence; the *Im*3*m*-Cub phase is difficult to be observed on cooling at ambient pressure because the high-temperature *Ia*3*d*-Cub phase is easily supercooled until the crystallization occurs.[2] As shown in Figures S4a and S4b, however, the two Cub phases were detected both on heating and on cooling under hydrostatic pressures up to around 50 MPa. Supercooling of the *Ia*3*d*-Cub phase was largely suppressed under pressures. The pattern for the *Im*3*m*-Cub phase and that for the *Ia*3*d*-Cub phase, both of which were observed at 20 MPa, are given in Figures S1e and S1f, respectively. At 50 MPa, the (001) reflection of the SmC(hp) phase was detected at 143 and 141 °C on cooling, with the coexistence of the *Im*3*m*-Cub phase and/or a crystalline (C_3) state; another crystalline (C_2) state appeared at 141 °C and grew when temperature was further decreased (Figure S4b). The crystalline phases C_3 and C_2 were often observed as spot-like oriented patterns, suggesting the oriented growth of the domains. Above 50 MPa, the *Im*3*m*-Cub phase disappeared both on heating and on cooling, and alternatively, the region of the SmC(hp) phase appeared and extended toward high temperatures with increasing pressure, showing an enantiotropic phase sequence of C_2 – C_3 – SmC(hp) – *Ia*3*d*-Cub – I; this phase sequence was observed between about 53 and 93 MPa, recognized as the intermediate-pressure region. Thus, from the low- to the intermediate-pressure regions, two phase sequences of the C_2 – *Im*3*m*-Cub – *Ia*3*d*-Cub – I and of C_2 – C_3 – SmC(hp) – *Ia*3*d*-Cub – I competitively exist. Figure 4c presents the plots of *d* spacings of observed reflections against temperature at 65 MPa. The spacings of the *Ia*3*d*-Cub (211) and (220) reflections at this pressure are clearly larger than the corresponding values at lower pressures such as 10 and 50 MPa. Such expansion of the *Ia*3*d*-Cub lattice at higher pressures is similarly observed for BABH-14. Beyond about 93 MPa, the *Ia*3*d*-Cub phase disappeared, showing an enantiotropic phase sequence of C_2 – C_3 – SmC(hp) – I. In Figure S4d, the plots of *d* spacings of observed reflections vs. temperature at 100 MPa are presented.

The temperature variation of XRD pattern was also measured for BABH-18 at various pressures and the *d* spacings of observed reflections vs. temperature plots are presented in Figure S5. The type of the Cub phase was mostly *Ia*3*d* type and the observed XRD patterns are presented in Figure S1g and S1h. Looking at Figure S5 closer, the formation was found to be pressure-dependent: At low pressures such as 30 MPa (Figure S5a), the *d* spacings of the (211) and (220) reflections showed almost no temperature dependence, but, at 51 MPa (Figure S5b), a negative temperature dependence was observed. The slope became steeper with increasing pressure, and most

prominent at around 70 MPa (Figure S5c). Furthermore, at this pressure, the *d* spacings of the *Ia*3*d*-Cub (211) and (220) reflections showed a bent at around 146 °C on cooling, changing to almost no temperature dependence, before the completion of crystallization. This suggests the formation of the *Im*3*m*-Cub phase; the two reflections may be assigned to its (321) and (420) reflections. The preliminary SAXS data obtained at SPring-8 facilities also supports the formation of this phase.[6] When pressure was elevated further to 90 MPa (Figure S5d) and to 120 MPa (Figure S5e), the slope of the *d* spacing vs. temperature curve for the *Ia*3*d*-Cub (211) and (220) reflections in turn became mild and the temperature region gradually contracted. At 90 MPa, as another feature around this pressure, the SmC(hp) phase region appeared and the phase sequence of Cr – SmC(hp) – *Ia*3*d*-Cub – I was observed as the behavior of the intermediate-pressure region between about 83 and 123 MPa. At about 140 MPa, only the SmC(hp) phase region remained (Figure S5f).

***T* – *P* phase diagrams for BABH-8, 10, and 12**.

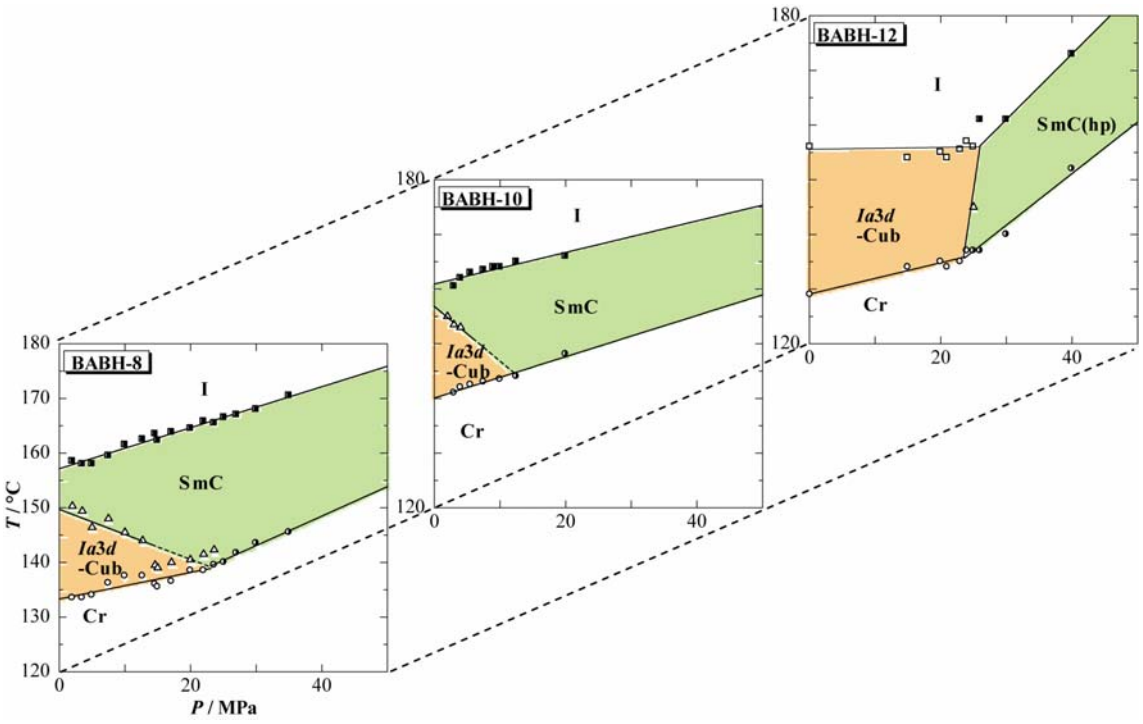

Fig. S6. *T-P* phase diagrams of BABH-8,[7] BABH-10[7] and BABH-12 established on the basis of their heating data; light brown and green regions represent the *Ia*3*d*-Cub and SmC (or alternatively, SmC(hp)) phase regions, respectively.

Quasi-binary picture model.[7]

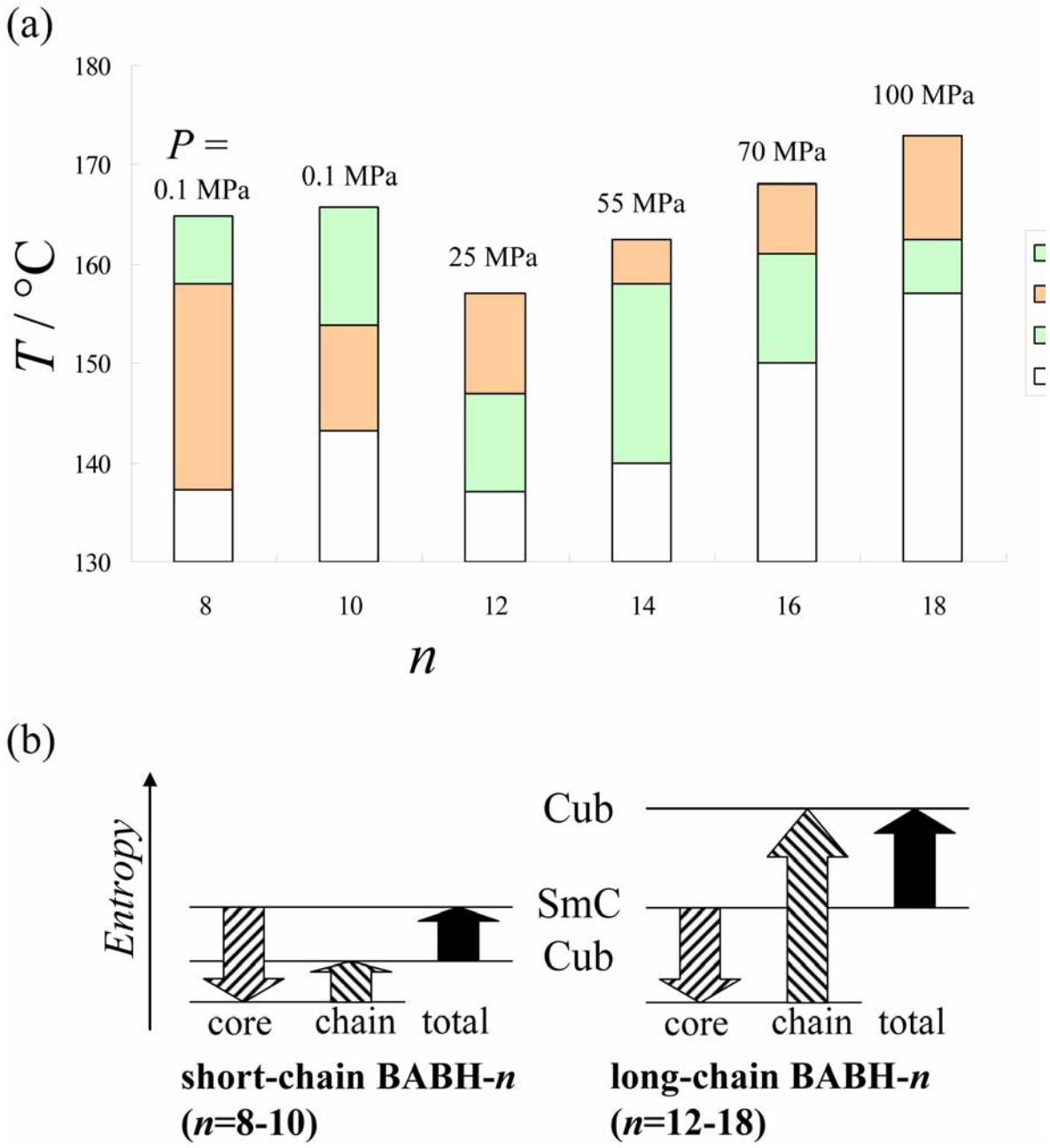

Fig. S7. (a) Inversion of phase sequence between the SmC and *Ia*3*d*-Cub phases with elongation of the alkyl chain, and (b) schematic representations of different contributions of the core and alkyl chain parts to the SmC-to-Cub transition entropy between the short- and long-chain BABHs.

Additional comments on hydrogen bonding fashions in BABH-n systems

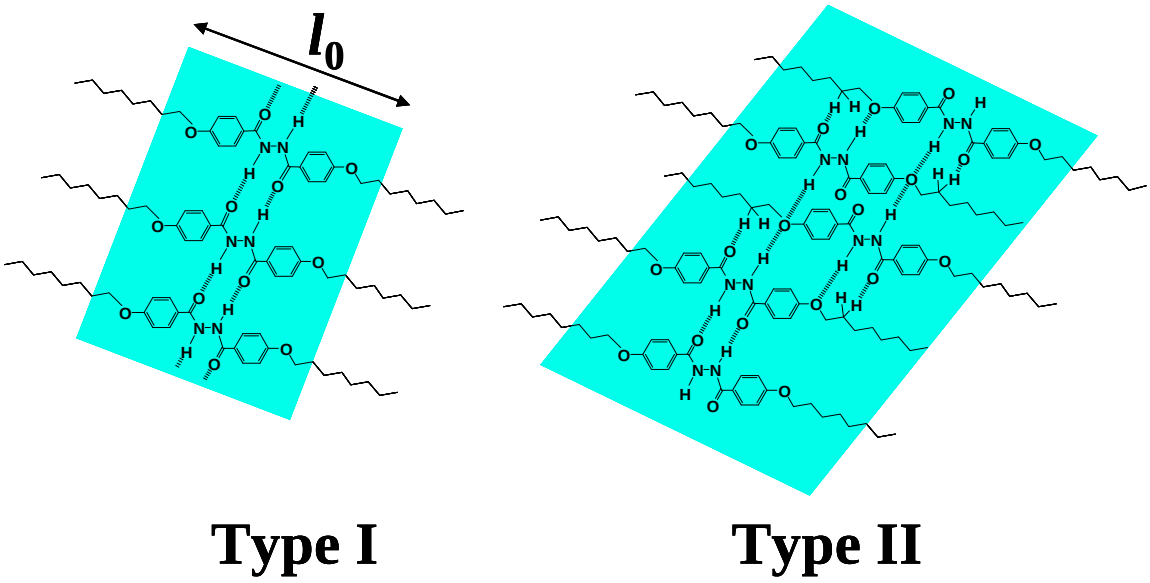

Fig. S8. Schematic representation of two aggregation modes,[8] Type I and II. See text for details.

As schematically illustrated in Fig. S11, one type of core aggregation, Type I, involves all the N-H groups being associated with the C=O groups via –N–H ··· O=C–, called "single-layered core" in our previous publication[8], and the other type, Type II, contains a bonding between the N-H group and the ether oxygen atom and a very weak bonding between the C=O group and the hydrogen in an alkyl chain in addition to the familiar –N–H ··· O=C– bonding. The latter type is called "double-layered cores", where mutual displacement of neighboring cores along the long molecular axis would lead to an increase in the effective core size, and also, weaker interactions would result in an apparent expansion of the core radius. In both Types I and II, of course, interactions themselves are actually dynamic, changing their counterparts to preserve fluidity, and thus, the above representation is an example of snapshots for the two core aggregations.

References

1 H. Mori, S. Kutsumizu, T. Ito, M. Fukatami, K. Saito, K. Sakajiri and K. Moriya, *Chem. Lett.* 2006, **35**, 362-363.

2 S. Kutsumizu, H. Mori, M. Fukatami, S. Naito, K. Sakajiri and K. Saito, *Chem. Mater.* 2008, **20**, 3675-3687.

3 K. Ozawa, Y. Yamamura, S. Yasuzuka, H. Mori, S. Kutsumizu and K. Saito, *J. Phys. Chem. B* 2008, **112**, 12179–12181.

4 Y. Maeda, H. Mori and S. Kutsumizu, *Liq. Cryst*. 2009, **36**, 217-223.

5 Y. Maeda, S. Kutsumizu and S. Sakurai, *Liq. Cryst*. 2012, **39**, 451-455.

6 S. Sakurai and S Kutsumizu, unpublished results.

7 Y. Maeda, H. Mori and S. Kutsumizu, *Liq. Cryst.* 2010, **37**, 463-473 and references therein.

8 Y. Nakazawa, Y. Yamamura, S. Kutsumizu and K. Saito, *J. Phys. Soc. Jpn.* 2012, **81**, 094601.